Higgs-strahlung production process $e^+e^- \to Zh$ at the future Higgs factory in the Minimal Dilaton Model

Junjie Cao,[a,b] **Zhaoxia Heng,**[a] **Dongwei Li,**[a] **Liangliang Shang**[a] **and Peiwen Wu**[c]

[a] *Department of Physics, Henan Normal University,*
Xinxiang 453007, China

[b] *Center for High Energy Physics, Peking University,*
Beijing 100871, China

[c] *State Key Laboratory of Theoretical Physics, Institute of Theoretical Physics, Academia Sinica,*
Beijing 100190, China

E-mail: junjiec@itp.ac.cn, zhaoxiaheng@gmail.com,
dongwhey@foxmail.com, shlwell1988@gmail.com, pwwu@itp.ac.cn

ABSTRACT: We investigate the Higgs-strahlung production process $e^+e^- \to Zh$ at the future Higgs factory such as TLEP by including radiative corrections in the Minimal Dilaton Model (MDM), which extends the SM by one singlet scalar called dilaton. We consider various theoretical and experimental constraints on the model, and perform fits to the Higgs data taken from ATLAS, CMS and CDF+D0. Then for the 1σ surviving samples, we calculate the MDM predictions on the inclusive production rate $\sigma(e^+e^- \to Zh)$ at the 240-GeV Higgs factory, and also the signal rates of $e^+e^- \to Zh$ with the Higgs boson decaying to $b\bar{b}$ and $\gamma\gamma$. We have following observations: (1) In the heavy dilaton scenario, the deviation of $\sigma(e^+e^- \to Zh)$ from its SM prediction can vary from -15% to 85%, which mainly arises from the modification of the tree-level hZZ coupling and also the radiative correction induced by possibly large Higgs self-couplings. (2) The processes $e^+e^- \to Zh$ at the Higgs factory and $pp \to hh$ at 14-TeV LHC are complementary in limiting the MDM parameter space. Requiring the deviation of $\sigma(e^+e^- \to Zh)$ from its SM prediction to be less than 1% and that of $\sigma(pp \to hh)$ to be less than 50%, $\tan\theta_S$ in the MDM will be limited to be $-0.1 < \tan\theta_S < 0.3$, and the deviations of the signal rates are constrained to be $|R_{b\bar{b}}| < 2\%$ and $|R_{\gamma\gamma}| < 7\%$. Especially, the Higgs self-coupling normalized to its SM prediction is now upper bounded by about 4. (3) In the light dilaton scenario, the deviation of $\sigma(e^+e^- \to Zh)$ may reach -7%, and requiring its size to be less than 1% will result in $0 < \tan\theta_S < 0.1$, and $-10\% < R_{b\bar{b}}, R_{\gamma\gamma} < 1\%$.

Contents

1   Introduction

In July 2012, the discovery of a new boson with mass around 125 GeV at the CERN Large
Hadron Collider (LHC) [1, 2] marked a great triumph in the history of particle physics.
With the growingly accumulated data, the properties of this newly discovered boson are
in excellent agreement with those of the Higgs boson predicted by the Standard Model
(SM), including the further measurements of its spin and parity quantum numbers [3–5].
However, up to now, there is no evidence to establish whether the Higgs sector contains
only one Higgs doublet. Instead, the Higgs-like resonance with mass about 125 GeV can
also be well explained in many new physics models, such as low energy supersymmetric
models [6–27] and the dilaton models [28–35].

So far various Higgs couplings to SM fermions and vector bosons based on the cur-
rent LHC data still have large uncertainties. Taking the hZZ coupling as an example,
the measured value normalized to its SM prediction is $1.43 \pm 0.33(\text{stat}) \pm 0.17(\text{syst})$ for
ATLAS result and 0.92 ± 0.28 for CMS result [36–39]. Nevertheless, at the future High
Luminosity LHC (HL-LHC) with 300 fb^{-1} (3000 fb^{-1}) integrated luminosity, the precision
of the C_{hZZ} measurement is expected to reach $4 - 6\%$ ($2 - 4\%$) [36–39]. Compared with
the hadron collider, the future e^+e^- collider may have a stronger capability in the C_{hZZ}
measurement through the Higgs-strahlung production $e^+e^- \rightarrow Zh$. For example, at the
proposed International Linear Collider (ILC) with collision energy up to 1TeV and luminos-
ity up to $1000\,fb^{-1}$, the precision may be improved to be near 0.5% [36–39]. And an even
more remarkable precision of 0.05% may be achieved at the recently proposed Triple-Large
Electron-Positron Collider (TLEP) [36–39], which is a new circular e^+e^- collider operated
at $\sqrt{s} = 240\,\text{GeV}$ with $10^4\,fb^{-1}$ integrated luminosity [40, 41].

The story of the Higgs self-coupling, however, is quite different. By now such a cou-
pling has basically not been constrained by the current Higgs data, while on the other
hand, it can be quite large in some new physics models such as the Minimal Dilaton Model
(MDM) [42–44]. Obviously, the next important task of experimentalists is to determine the

coupling size as precise as possible, which is essential in reconstructing the Higgs potential and consequently determining the mechanism of the electro-weak symmetry breaking. At both the LHC and the ILC, the Higgs self-coupling can be measured directly through the Higgs pair production [45–59]. The recent studies suggest that a precision of 50% for the coupling can be obtained through $pp \to hh \to bb\gamma\gamma$ at the HL-LHC with an integrated luminosity of 3000 fb^{-1} [36–39, 60–64], and it may be further improved to be around 13% at the ILC with collision energy up to 1TeV [36–39].

One interesting feature of the Higgs-strahlung production $e^+e^- \to Zh$ is that, while at tree level its rate is solely determined by the C_{hZZ} coupling, at loop level the rate also depends on the Higgs self-coupling and may be significantly altered by such a coupling. This brings us the possibility that apart from the direct Higgs pair production, the Higgs self-coupling may also be measured indirectly from the process $e^+e^- \to Zh$ with the e^+e^- collision energy below the di-Higgs threshold. As shown in [65], given that the inclusive cross section $\sigma(e^+e^- \to Zh)$ is measured with a precision of 0.4% at the TLEP [40, 41], the Higgs self-coupling may be constrained to an accuracy of 28%.

In this work we take the MDM as an example to investigate the Higgs-strahlung production $e^+e^- \to Zh$ by including radiative corrections. We scan the MDM parameters by considering various experimental and theoretical constraints. Then for the surviving samples we calculate their predictions on $\sigma(e^+e^- \to Zh)$ at the 240-GeV TLEP, and investigate to what extent the parameters will be constrained given the future precision of the cross section measurement. Noting that more observables will be helpful to further limit the parameter space, we also perform a study on the signals of the Higgs-strahlung production with the Higgs boson decaying to $\gamma\gamma$ or $b\bar{b}$. We note that similar study has been done in supersymmetric models [66].

This work is organized as follows. In section II, we briefly review the MDM and experimental and theoretical constraints on it. Then we calculate $\sigma(e^+e^- \to Zh)$ by including radiative corrections and discuss the capability of the Higgs factory to determine the model parameters in section III. Finally, we summarize our conclusions in section IV.

2   The Minimal Dilaton Model

The MDM is an extension of the SM by introducing a linearized singlet dilaton field S and a vector-like top partner T with the same quantum number as the right-handed top quark. The low energy effective Lagrangian of the MDM is given by [42–44]

$$\mathcal{L} = \mathcal{L}_{\text{SM}} - \frac{1}{2}\partial_\mu S \partial^\mu S - \frac{m_S^2}{2}S^2 - \frac{\lambda_S}{4!}S^4 - \frac{\kappa}{2}S^2 |H|^2 - m_H^2 |H|^2 - \frac{\lambda_H}{4} |H|^4$$
$$- \bar{T}\left(\slashed{D} + \frac{M}{f}S\right)T - \left[y'\overline{T}_R(q_{3L} \cdot H) + \text{h.c.}\right], \tag{2.1}$$

where $\mathcal{L}_{\text{SM}}$ is the part of the SM Lagrangian without the Higgs potential, M represents the scale of a certain strong dynamics in which the fields T and S are involved, q_{3L} is the $SU(2)_L$ left-handed quark doublet of the third generation, and M_H, M_S, λ_S, κ and λ_H are all free parameters describing the new Higgs potential. The singlet dilaton field S and

the doublet Higgs field H will mix with each other, which can be parameterized by the Higgs-dilaton mixing angle θ_S as

$$S = f + h \sin\theta_S + s \cos\theta_S,$$

$$H = \begin{pmatrix} \phi^+ \\ \frac{1}{\sqrt{2}}(v + h\cos\theta_S - s\sin\theta_S + i\phi^0) \end{pmatrix} \tag{2.2}$$

with f and $v = 246\,\mathrm{GeV}$ being the vacuum expectation values (vev) of S and H respectively, h and s denoting the mass eigenstates of the Higgs boson and the dialton, and ϕ^0 and ϕ^+ representing the Goldstone bosons. Similarly, q_{3L}^u and T will mix to form mass eigenstates t and t' so that

$$q_{3L}^u = \cos\theta_L t_L + \sin\theta_L t'_L,$$

$$T_L = -\sin\theta_L t_L + \cos\theta_L t'_L. \tag{2.3}$$

If θ_S, f and physical masses m_h, m_s are taken as the input of the theory, one can re-express the dimensionless parameters λ_S, κ and λ_H as follows [44]

$$\lambda_S = \frac{3|m_h^2 - m_s^2|}{2f^2}\left[\frac{m_h^2 + m_s^2}{|m_h^2 - m_s^2|} - \mathrm{Sign}(\sin 2\theta_S)\cos 2\theta_S\right],$$

$$\kappa = \frac{|m_h^2 - m_s^2|}{2fv}|\sin 2\theta_S|,$$

$$\lambda_H = \frac{|m_h^2 - m_s^2|}{v^2}\left[\frac{m_h^2 + m_s^2}{|m_h^2 - m_s^2|} + \mathrm{Sign}(\sin 2\theta_S)\cos 2\theta_S\right]. \tag{2.4}$$

In this case, the trilinear interactions among h, s, ϕ^0 and $\phi^\pm$ are given by

$$C_{hhh} = v\left[\frac{3}{2}\lambda_H\cos^3\theta_S + \lambda_S\eta^{-1}\sin^3\theta_S + 3\kappa(\cos\theta_S\sin^2\theta_S + \eta^{-1}\cos^2\theta_S\sin\theta_S)\right], \tag{2.5}$$

$$C_{hss} = v\left[\kappa(\cos^3\theta_S + \eta^{-1}\sin^3\theta_S) + \left(\frac{3}{2}\lambda_H - 2\kappa\right)\cos\theta_S\sin^2\theta_S \right.$$
$$\left. + \eta^{-1}(\lambda_S - 2\kappa)\cos^2\theta_S\sin\theta_S\right], \tag{2.6}$$

$$C_{hhs} = v\left[\kappa(-\sin^3\theta_S + \eta^{-1}\cos^3\theta_S) - \left(\frac{3}{2}\lambda_H - 2\kappa\right)\sin\theta_S\cos^2\theta_S \right.$$
$$\left. + \eta^{-1}(\lambda_S - 2\kappa)\sin^2\theta_S\cos\theta_S\right], \tag{2.7}$$

$$C_{h\phi^0\phi^0} = v\left(\kappa\eta^{-1}\sin\theta_S + \frac{\lambda_H}{2}\cos\theta_S\right), \tag{2.8}$$

$$C_{h\phi^+\phi^-} = v\left(\kappa\eta^{-1}\sin\theta_S + \frac{\lambda_H}{2}\cos\theta_S\right) \tag{2.9}$$

with $\eta \equiv \frac{v}{f}$, and the normalized couplings of h and s with Z or ϕ^0 are given by

$$C_{hZZ}/SM = C_{hZ\phi^0}/SM = \cos\theta_S, \quad C_{sZZ}/SM = C_{sZ\phi^0}/SM = -\sin\theta_S,$$

$$C_{hhZZ}/SM = \cos^2\theta_S, \quad C_{hsZZ}/SM = -\cos\theta_S\sin\theta_S, \quad C_{ssZZ}/SM = \sin^2\theta_S. \tag{2.10}$$

In the following we differentiate two scenarios according to the dilaton mass [44]:

- Heavy dilaton scenario: $m_s > m_h$. An important feature of this scenario is that the trilinear Higgs self-coupling C_{hhh} may be very large.

- Light dilaton scenario: $m_s < m_h/2 \simeq 62\,\mathrm{GeV}$. In this scenario, the Higgs exotic decay $h \to ss$ is open with a possible large branching ratio, so it may be tightly constrained by current Higgs data.

We here do not consider the possibility of $m_h/2 \le m_s \le m_h$ because we checked that such a possibility has no distinct features, and is therefore less interesting from phenomenology point of view. For both the light and heavy dilation scenarios, we consider the constraints similar to what we did in [44], which are given by

(1) Vacuum stability of the scalar potential and absence of the Landau pole up to 1TeV.

(2) Bounds from the search for Higgs-like scalar at LEP, Tevatron and LHC.

(3) $m_{t'} \ge 1\mathrm{TeV}$ as suggested by the LHC search for top quark partner [67–69] and constraints from the precision electroweak data [42]. With this constraint, we have $\cos\theta_L > 0.97$ and consequently $C_{htt}/SM \simeq \cos\theta_S$ [44].

(4) Constraints from the measured Higgs properties. In implementing this constraint, we use the combined data (22 sets) from ATLAS, CMS and CDF+D0 and perform a fit with the same method as that in [70–72]. We obtained $\chi^2_{\min} = 18.66$ in the MDM, which is less than χ^2 for the SM ($\chi^2_{SM} = 18.79$), and paid particular attention to 1σ samples in the fit.

As shown in [44], parameter points satisfying the above constraints will predict $\cos\theta_S > 0.92$, and $C_{h\bar{t}'t'}/C^{SM}_{h\bar{t}t} < 0.1$. As will be seen below, this feature is beneficial for our analysis.

3 Calculations and numerical results

In the SM, the radiative corrections to the Higgs-strahlung production process $e^+e^- \to Zh$ come from the Z boson self-energy, the vertex corrections to Ze^+e^-, he^+e^-, ZZh and $Z\gamma h$ interactions, and also box contributions [73, 74]. The full calculation of these corrections is quite complex (e.g. more than sixty diagrams need to be calculated) and it was shown recently that the total weak correction is 5% for $m_h = 125\mathrm{GeV}$ and $\sqrt{s} = 240\mathrm{GeV}$ [75]. About the corresponding corrections in the MDM, we have following observations after comparing carefully the SM correction presented in [73]

- Although the contribution induced by the Higgs self-coupling is only 2% in the SM [75], it is potentially large in the MDM since the self-couplings among the scalars may be greatly enhanced [44]. In this work, we call such a contribution Type-I correction and will mainly discuss its effect on the production process in the following. The Feynman diagrams for such a correction are presented in figure 1.
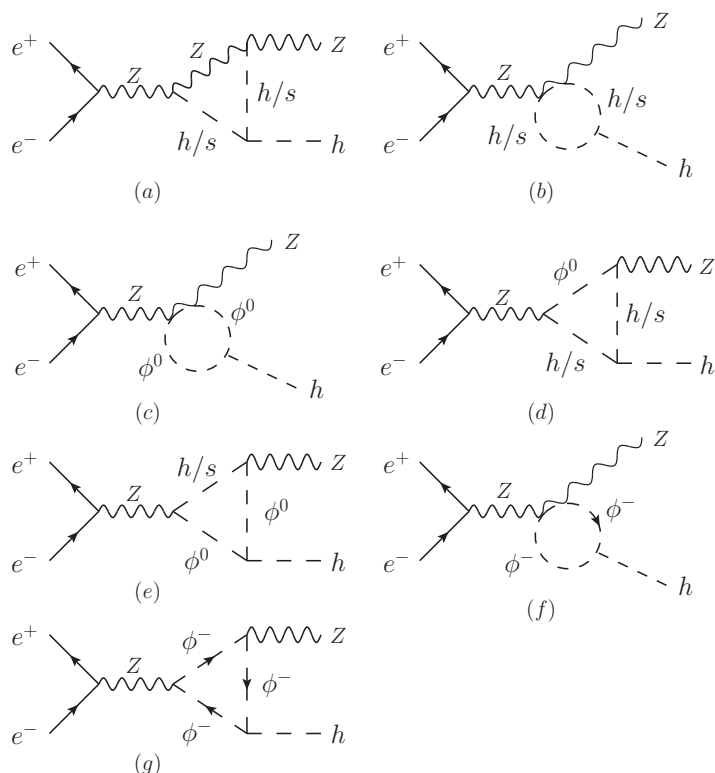
Figure 1. Feynman diagrams for the Higgs-strahlung production $e^+e^- \to Zh$ in the MDM with the radiative corrections coming from the Higgs self-couplings in the Feynman-'t Hooft gauge.
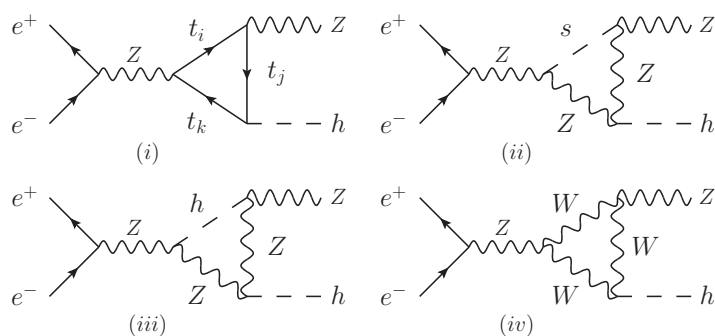
Figure 2. Representative Feynman diagrams for different types of contributions to the strahlung production in the MDM. Diagram (i) denotes t'-induced vertex correction to ZZh interaction if the particles in the loop contain at least one t'. Diagram (ii) represents the contribution that involves the sZZ interaction and meanwhile does not involve possible large self-couplings among the scalars. Diagram (iii) and diagram (iv) represents the Type-II and Type-III corrections respectively. For the Type-II contribution, it can be obtained from the corresponding SM result by scaling a factor of $\cos^3 \theta_S$, while for the Type-III contribution, it is obtained by scaling a factor of $\cos \theta_S$.

- The correction induced by t' should be much smaller than that of top quark since t' is heavy and meanwhile $C_{h\bar{t}'t'}$ is suppressed. Explicitly speaking, we find by calculation that, in the G_μ parametrization discussed in [73], the size of the correction is only about 0.35% in optimal case, which occurs for $m_{t'} \simeq 1010\text{GeV}$, $\sin\theta_L \simeq 0.24$ (corresponding to $y' \simeq 1.37$) and $\cos\theta_S \simeq 1$. In getting the correction, we compute not only the vertex correction to ZZh interaction with the Feynman diagram shown in panel (i) of figure 2, but also the self energies of SM gauge bosons and the Higgs boson to get the expressions of the counter terms, which are needed to renormalize the ZZh interaction [73]. Therefore the calculation process is rather complicated. We checked that our results are free of ultraviolet divergence. We also checked that the sample predicting a relatively large correction also predicts moderate large electro-weak precision data. So the precise extraction of the data at the TLEP and the future search for t' at the LHC can further limit the correction.

In our following discussion, we do not take such a correction into account since it affects little on our conclusions.

- For loops that involve the sZZ interaction and meanwhile do not involve possible large self-couplings among the scalars (see e.g. diagram (ii) in figure 2), we find that their contributions are less than 0.05% due to the singlet-dominated nature of the dilaton. In our discussion, we neglect such corrections.

- For the rest contributions, they can be categorized into Type-II correction and Type-III correction with their representative Feynman diagrams given in diagram (iii) and (iv) of figure 2 respectively. The Type-II correction arises from the Feynman diagrams where the field h appears in the loop and meanwhile the self-couplings among the scalars are not involved, so its expression can be obtained from the corresponding SM prediction by scaling a factor of $\cos^3\theta_S$. While the Type-III correction comes from the Feynman diagrams which involve the interaction of h with W, Z or SM fermions only once, and therefore its expression is obtained from the corresponding SM prediction by scaling a factor of $\cos\theta_S$.

In actual calculation, it is not easy to get directly the size of the Type-III correction since more than fifty diagrams are needed to compute. However, we note that the total weak correction to the Higgs-strahlung production in the SM is 5% [75], and meanwhile that the correction is composed by Type-I correction which is about 2% by our calculation, Type-II correction which is about -0.4% by our calculation, and also Type-III correction. Therefore, we infer that the Type-III correction in the SM is about 3.4%.

Based on above discussion, we conclude that the deviation of the inclusive production rate $\sigma(e^+e^- \to Zh)$ from its SM prediction, which is generally called genuine new physics contribution, is given by

$$R \equiv \frac{\sigma_{\text{MDM}}^{\text{LOOP}}(e^+e^- \to Zh) - \sigma_{\text{SM}}^{\text{LOOP}}(e^+e^- \to Zh)}{\sigma_{\text{SM}}^0(e^+e^- \to Zh)}$$

$$\simeq \cos^2\theta_S + 0.034\cos^2\theta_S - 0.004\cos^4\theta_S + \frac{\delta\sigma_{\mathrm{MDM}}^{\mathrm{scalar}}(e^+e^- \to Zh)}{\sigma_{\mathrm{SM}}^0(e^+e^- \to Zh)} - 1.05$$

$$\simeq 1.03\cos^2\theta_S + \frac{\delta\sigma_{\mathrm{MDM}}^{\mathrm{scalar}}(e^+e^- \to Zh)}{\sigma_{\mathrm{SM}}^0(e^+e^- \to Zh)} + 0.001\sin^2 2\theta_S - 1.05$$

$$\simeq 1.03\cos^2\theta_S + \frac{\delta\sigma_{\mathrm{MDM}}^{\mathrm{scalar}}(e^+e^- \to Zh)}{\sigma_{\mathrm{SM}}^0(e^+e^- \to Zh)} - 1.05 \tag{3.1}$$

where $\sigma_{\mathrm{MDM}}^{\mathrm{LOOP}}$ and $\sigma_{\mathrm{SM}}^{\mathrm{LOOP}}$ are the cross sections at one loop level in the MDM and the SM respectively, σ_{SM}^0 is the SM prediction on the cross section at tree level, and $\delta\sigma_{\mathrm{MDM}}^{\mathrm{scalar}}$ denotes the correction induced by the self-couplings among the scalars with the corresponding diagrams given in figure 1. Note that the first term on the right hand of the second equation corresponds to the tree-level contribution, which differs from its SM prediction due to the modified hZZ coupling by a factor $\cos\theta_S$, and the second and third terms correspond the interferences of the Type-III correction and the Type-II correction with the tree-level amplitude respectively. Also note that the constraints have required $\cos\theta_S > 0.92$, so the deviation R mainly arises from the modification of the tree-level hZZ coupling and $\delta\sigma_{\mathrm{MDM}}^{\mathrm{scalar}}$.

In this work, we take $m_Z = 91.19\,\mathrm{GeV}$, $\alpha = 1/128$ [76] and $m_h = 125\,\mathrm{GeV}$, and fix the e^+e^- collision energy at $240\,\mathrm{GeV}$. We obtained $\sigma_{SM}^0(e^+e^- \to Zh) = 236\,fb$, which is in accordance with the result in [40, 41]. In our calculations of $\delta\sigma_{\mathrm{MDM}}^{\mathrm{scalar}}$, we adopt the Feynman-'t Hooft gauge, and therefore the diagram involving the Goldstone fields must be considered. Moreover, we note from figure 1 that, except for the dilaton mass, the masses of the particles in the loops are fixed, and meanwhile, since the dilaton coupling with Z boson is very small due to its singlet-dominated nature, its induced contribution should be relatively small if C_{hss} or C_{hhs} is not much larger than C_{hhh}. These features imply that $\delta\sigma_{\mathrm{MDM}}^{\mathrm{scalar}}$ or R can be expressed in a semi-analytic way, which is given by

$$R \simeq 1.03\cos^2\theta_S + 0.02 \times \cos\theta_S \times \frac{C_{hhh}}{\mathrm{SM}} + 0.000146 \times \left(\frac{C_{hhh}}{\mathrm{SM}}\right)^2 - 1.05. \tag{3.2}$$

In above equation, the second term on the right side reflects the interference between the tree-level contribution and the correction from the self-couplings, and the third represents the pure self-coupling contribution which can not be neglected if $C_{hhh}/SM \gg 1$. For the results presented below, we obtain the value of $\delta\sigma_{\mathrm{MDM}}^{\mathrm{scalar}}$ by exact calculation, and we checked that for nearly all the 1σ samples, eq. (3.2) is a good approximation.

### 3.1 Numerical results in the heavy dilaton scenario

For the heavy dilaton scenario, we consider the constraints listed in section II and scan the relevant parameters in the following ranges like what we did in [44]

$$1 \leq \eta^{-1} < 10, \quad 130\ \mathrm{GeV} < m_s < 1\ \mathrm{TeV}, \quad |\tan\theta_S| < 2, \quad 1\mathrm{TeV} < m_{t'} < 3\mathrm{TeV}. \tag{3.3}$$

Then we investigate the properties of the 1σ samples, which satisfy $\chi^2 - \chi_{\mathrm{min}}^2 \leq 2.3$.

In figure 3 we project the 1σ samples on the plane of C_{hhh}/SM versus $\cos\theta_S$ and also show some lines corresponding to specific values of R calculated from eq. (3.2). One can learn the following features:
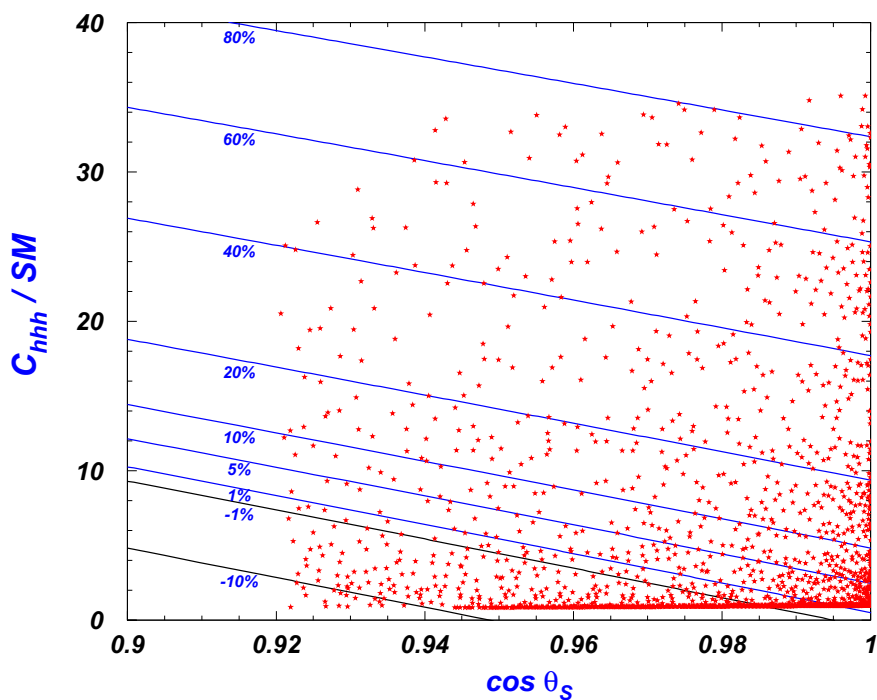
Figure 3. The scatter plot of the 1σ samples in the heavy dilaton scenario, projected on the plane of C_{hhh}/SM versus $\cos\theta_S$. The lines denote various specific values of the deviation R calculated from eq. (3.2).
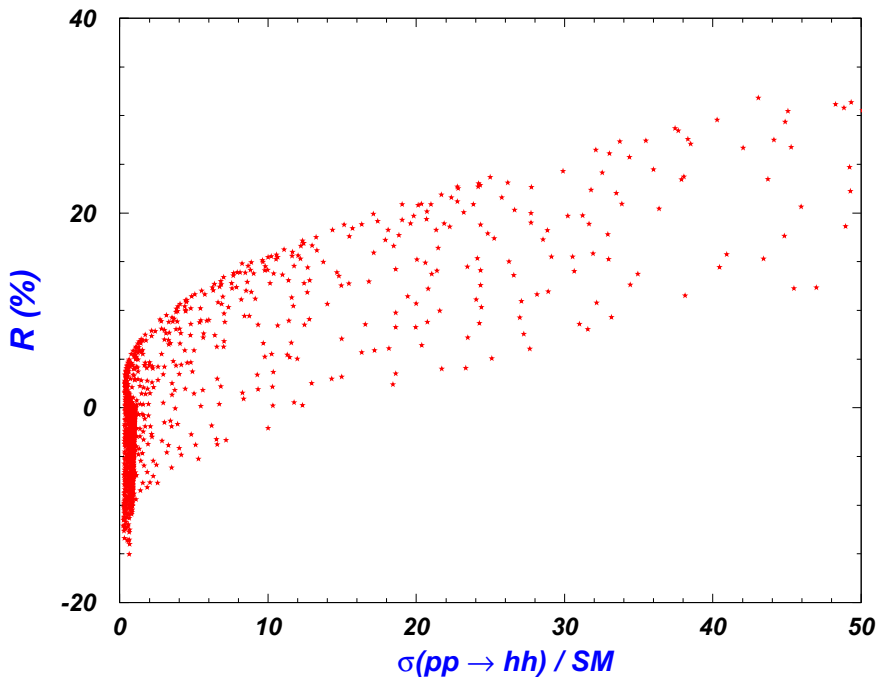
Figure 4. Same as figure 3, but projected on the plane of R versus the normalized cross section rate $\sigma(pp \to hh)/SM$ at the 14-TeV LHC.

- Due to the small coefficients of the second and third terms in eq. (3.2), a given value of R in eq. (3.2) corresponds to a very prolate ellipse on the whole plane of C_{hhh}/SM versus $\cos\theta_S$. For $\cos\theta_S > 0.92$, the ellipse curves turn out to be nearly straight lines in figure 3.

- As indicated by eq. (3.2), the tree-level modification of the hZZ coupling is to decrease the inclusive rate, while the effect of the correction induced by the self-couplings is to increase the rate. For the 1σ samples considered, the deviation R varies from -15% to 85%. Such possible large deviation is due to a large uncertainty in determining the hZZ coupling from current Higgs data as well as currently a very weak constraint on the self-couplings.

  Obviously, if R is moderately large, two loop or higher order corrections should also be taken into account.

With the upgraded energy and luminosity of the LHC, C_{hhh} may be measured directly through the Higgs pair production since it affects the production rate through the parton process $gg \to h^* \to hh$. As shown in figure 6 of [44], for $C_{hhh}/SM \gtrsim 2.5$ in the heavy dilaton scenario of the MDM, the normalized cross section $\sigma(pp \to hh)/SM$ at the 14-TeV LHC increases monotonically as C_{hhh}/SM becomes larger. In order to compare the effect of the Higgs self-coupling at the LHC with that at the future Higgs factory, we show the correlation of $\sigma(pp \to hh)$ at the 14-TeV LHC with $\sigma(e^+e^- \to Zh)$ at 240-GeV TLEP in figure 4. This figure manifests that a $\sigma(pp \to hh)/SM$ of several tens usually corresponds to a R larger than 5%. For example, in the case of $\sigma(pp \to hh)/SM = 40$, R varies from 10% to 30%. While on the other hand, even for $\sigma(pp \to hh)/SM \sim 1$, the size of R may still be moderately large, changing from -15% to 5%. These features tell us that the processes $pp \to hh$ and $e^+e^- \to Zh$ are complementary in limiting the parameters of the MDM.

In order to investigate the capability of the future experiments to detect the parameter space of the MDM, we assume measurement precisions of 50% for $\sigma(pp \to hh)$ at 14 TeV [36–39, 60–64] and 1.0% for $\sigma(e^+e^- \to Zh)$ at 240 GeV [40, 41]. Then we project all the 1σ samples, the 1σ samples that further satisfy $|\sigma(pp \to hh)/SM-1| \leq 50\%$ and the 1σ samples satisfying both $|\sigma(pp \to hh)/SM-1| \leq 50\%$ and $|R| \leq 1.0\%$ on the plane of η^{-1} versus $\tan\theta_S$ in the left panel, the middle panel and the right panel of figure 5, respectively. This figure indicates that $\tan\theta_S$ is allowed to be within $-0.4 \leq \tan\theta_S \leq 0.4$ for the 1σ samples without any further requirement, and is reduced to the region $-0.1 \leq \tan\theta_S \leq 0.3$ after the LHC and TLEP measurements. Moreover, we checked that, in comparison with the number of the samples in the left panel, the numbers in the middle and right panels are reduced by about 40% and more than 80% respectively. We also checked that the samples in the right panel satisfy $0.98 \leq C_{hhh}/SM \leq 4.4$. These facts reflect the great power of the future experiments in limiting the MDM.

Since the MDM parameters can still survive in a fairly wide region after considering the measurement of the inclusive production rate at future Higgs factory, we need to consider more observables to limit the model. So we also investigate the signal rates of $e^+e^- \to Zh \to Zb\bar{b}, Z\gamma\gamma$. Similar to R, we define the deviations of the signal rates from
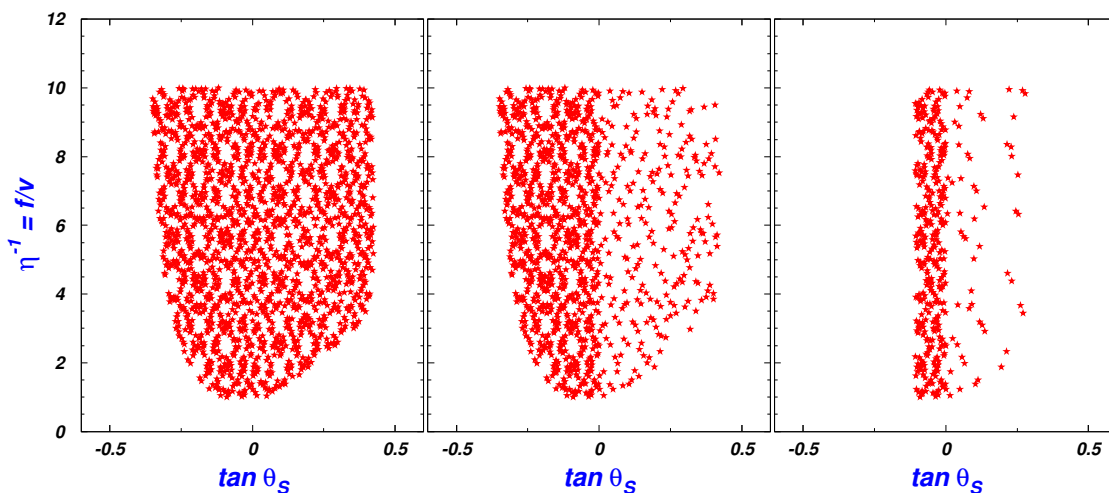
Figure 5. Same as figure 3, but projected on the plane of $\eta^{-1} = f/v$ versus $\tan\theta_S$. Samples shown in the left panel, the middle panel and the right panel correspond to the total 1σ samples, the 1σ samples that further satisfy $|\sigma(pp \to hh)/SM - 1| < 50\%$ and the 1σ samples satisfying both $|R| < 1.0\%$ and $|\sigma(pp \to hh)/SM - 1| < 50\%$, respectively.
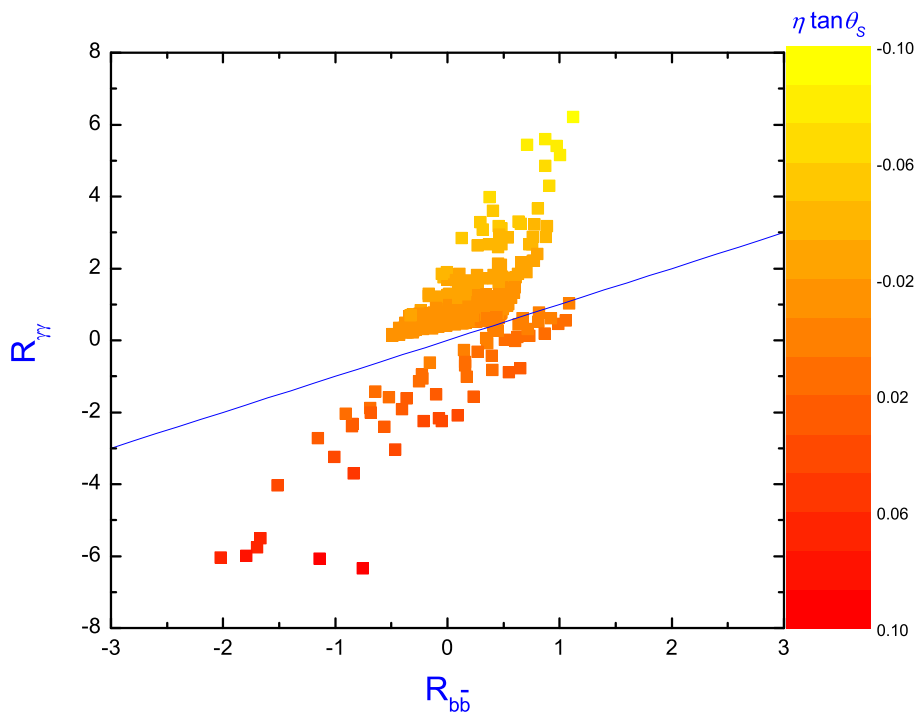
Figure 6. Samples in the right panel of figure 5, but projected on the plane of $R_{\gamma\gamma}$ versus $R_{b\bar{b}}$, where dependence on $\eta \tan\theta_S$ is also shown. For clarity, we draw a blue line corresponding to $R_{b\bar{b}} = R_{rr}$.

their SM predictions by

$$R_{b\bar{b}} \equiv \frac{\sigma_{\mathrm{MDM}}^{\mathrm{LOOP}}(e^+e^- \to Zh)Br_{\mathrm{MDM}}(h \to b\bar{b}) - \sigma_{\mathrm{SM}}^{\mathrm{LOOP}}(e^+e^- \to Zh)Br_{\mathrm{SM}}(h \to b\bar{b})}{\sigma_{\mathrm{SM}}^0(e^+e^- \to Zh)Br_{\mathrm{SM}}(h \to b\bar{b})},$$

$$R_{\gamma\gamma} \equiv \frac{\sigma_{\mathrm{MDM}}^{\mathrm{LOOP}}(e^+e^- \to Zh)Br_{\mathrm{MDM}}(h \to \gamma\gamma) - \sigma_{\mathrm{SM}}^{\mathrm{LOOP}}(e^+e^- \to Zh)Br_{\mathrm{SM}}(h \to \gamma\gamma)}{\sigma_{\mathrm{SM}}^0(e^+e^- \to Zh)Br_{\mathrm{SM}}(h \to \gamma\gamma)} \quad (3.4)$$

where $Br_{MDM}(h \to b\bar{b})$ and $Br_{SM}(h \to b\bar{b})$ denote the branching ratio of $h \to b\bar{b}$ in the MDM and the SM respectively, and similar notation is applied for $h \to \gamma\gamma$. In the heavy dilaton scenario, $R_{b\bar{b}}$ and $R_{\gamma\gamma}$ can be approximated by [44]

$$R_{b\bar{b}} \simeq (R + 1.05) \cdot \frac{\cos^2 \theta_S \Gamma_{SM}^{b\bar{b}}}{\cos^2 \theta_S \Gamma_{SM}} \frac{\Gamma_{SM}}{\Gamma_{SM}^{b\bar{b}}} - 1.05 \simeq R, \quad (3.5)$$

$$R_{\gamma\gamma} \simeq (R + 1.05) \cdot (1 - 0.27\eta \tan \theta_S)^2 - 1.05 \quad (3.6)$$

where Γ_{SM} and $\Gamma_{SM}^{b\bar{b}}$ denote respectively the total width of the Higgs boson and the partial width of $h \to b\bar{b}$ in the SM. Note that the above approximations are good only for a sufficiently large R, but anyhow, they are helpful to understand our results. In figure 6, we project the samples in the right panel of figure 5 on the plane of $R_{\gamma\gamma}$ versus $R_{b\bar{b}}$ for different values of $\eta \tan \theta_S$. This figure indicates that $R_{b\bar{b}}$ is basically constrained in the range of $|R_{b\bar{b}}| < 2\%$, while $|R_{\gamma\gamma}|$ can maximally reach 7%. Considering that the expected precisions of measured $\sigma \cdot BR(h \to b\bar{b})$ and $\sigma \cdot BR(h \to \gamma\gamma)$ at 240-GeV TLEP can reach the level of 0.2% and 3.0% respectively [36–39], one can expect that by the measurement of the $b\bar{b}$ and $\gamma\gamma$ signal rates, one can get additional information about $\eta \tan \theta_S$ if the MDM is a correct theory.

3.2 Numerical results in the light dilaton scenario

In the light dilaton scenario we scan following parameter ranges by considering the constraints listed in section II

$$1 \leq \eta^{-1} < 10, \quad 0 \text{ GeV} < m_s < 62 \text{ GeV}, \quad |\tan \theta_S| < 2, \quad 1\text{TeV} < m_{t'} < 3\text{TeV}, \quad (3.7)$$

and investigate the properties of the 1σ samples, which are now defined by $\chi^2 - \chi^2_{\min} \leq 1.0$ [44]. Compared with the heavy dilaton scenario, the light dilaton scenario has two distinct features. Firstly, the Higgs exotic decay $h \to ss$ is open with a possible large branching ratio. So this scenario is more tightly constrained by current Higgs data. Secondly, the Higgs self-coupling strength C_{hhh}/SM is relatively small, around at either 1 or 0. As a result, the deviation R mainly comes from the modified hZZ coupling, so $R \simeq \cos^2 \theta_S - 1$. In figure 7 we project the 1σ samples on the plane of deviation R versus $\cos \theta_S$. As expected, the size of the deviation R monotonically decreases as $\cos \theta_S$ approaches 1, and it can maximally reach 7%. This figure also shows that there are two separated regions of R. We checked that it is due to the discontinuousness of C_{hhh}/SM, that is, the upper region corresponds to $C_{hhh}/SM \simeq 1$, while the lower region corresponds to $C_{hhh}/SM \simeq 0$.

Adopting the same analysis as figure 5, we show the 1σ samples projected on the plane of $\eta^{-1} = f/v$ versus $\tan \theta_S$ in figure 8, where the left panel shows all 1σ samples, while for
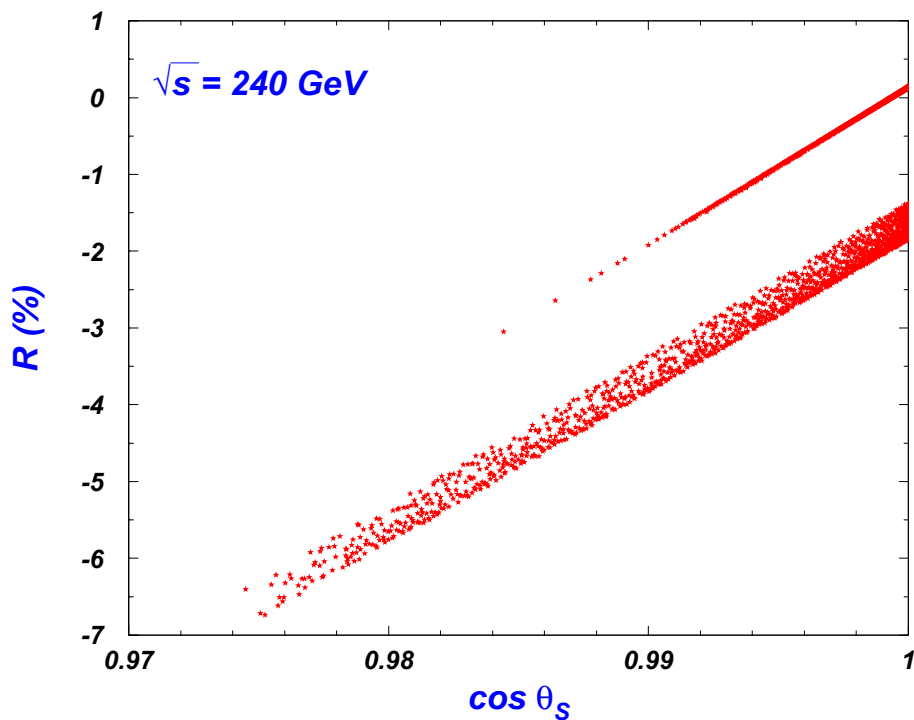
Figure 7. The scatter plot of the 1σ samples in the light dilaton scenario, projected on the plane of the deviation R versus $\cos\theta_S$.
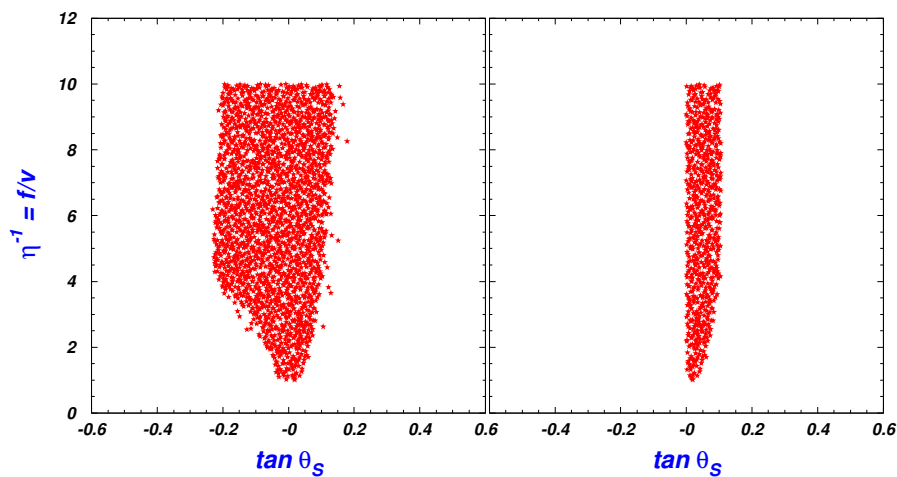
Figure 8. Scatter plot of the 1σ samples in the light dilaton scenario, projected on the plane of $\eta^{-1} = f/v$ versus $\tan\theta_S$. The left panel shows all 1σ samples, while the right panel shows samples further satisfying $|R| < 1.0\%$.
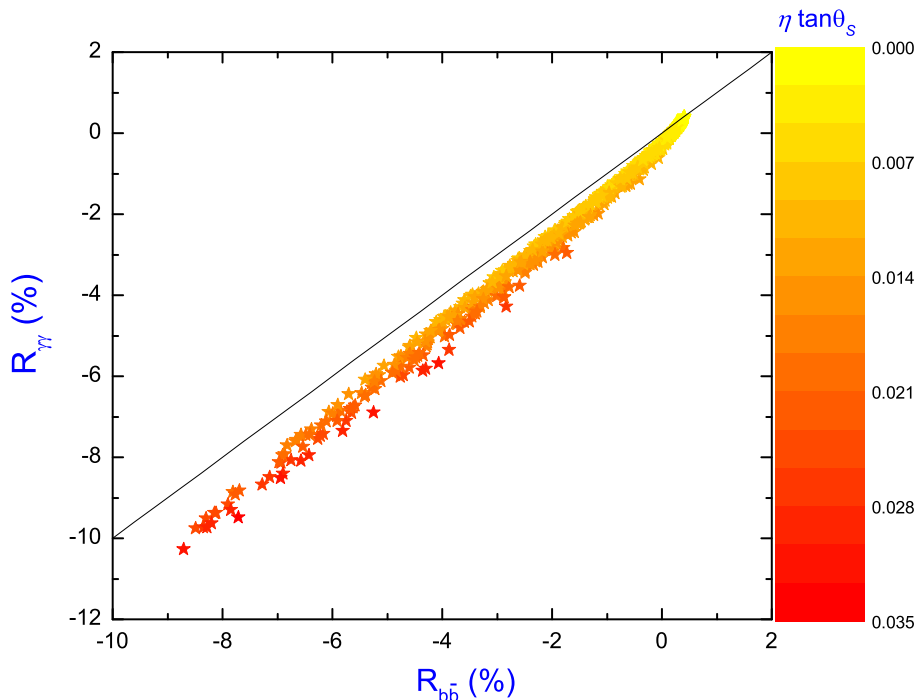
Figure 9. Same as figure 7, but projected on the plane of $R_{\gamma\gamma}$ versus $R_{b\bar{b}}$, and also shows the dependence on $\eta \tan\theta_S$.

comparison the right panel shows samples that further satisfy the requirement $|R| < 1.0\%$. Here we do not consider the deviation of $\sigma(pp \to hh)$ because it is very small in the light dilation scenario [44]. Figure 8 clearly shows that the MDM parameter space in the light dilaton scenario is also strongly constrained resulting in $0 < \tan\theta_S < 0.1$, in contrast with $-0.24 < \tan\theta_S < 0.2$ without the requirement of $|R| < 1.0\%$. Moreover, we checked that after the requirement, the number of the 1σ samples in the left panel of figure 8 is reduced by more than 70%.

Similar to what we did in the heavy dilaton scenario, we also investigate the signal deviations $R_{b\bar{b}}$ and $R_{\gamma\gamma}$, which can now be expressed as

$$R_{b\bar{b}} \simeq (R + 1.05)\frac{\cos^2\theta_S \Gamma_{SM}^{b\bar{b}}}{\cos^2\theta_S \Gamma_{SM} + \Gamma_{ss}}\frac{\Gamma_{SM}}{\Gamma_{SM}^{b\bar{b}}} - 1.05$$

$$\simeq (R + 1.05)(1 - Br(h \to ss)) - 1.05 \qquad (3.8)$$

$$R_{\gamma\gamma} \simeq (R + 1.05)(1 - 0.27\eta \tan\theta_S)^2(1 - Br(h \to ss)) - 1.05, \qquad (3.9)$$

where Γ_{ss} is the width of $h \to ss$ in the MDM, and we assume $\Gamma_{MDM} \equiv \cos^2\theta_S \Gamma_{SM} + \Gamma_{ss} \simeq \cos^2\theta_S \Gamma_{SM} \gg \Gamma_{ss}$. In figure 9 we show the relationship between $R_{\gamma\gamma}$ and $R_{b\bar{b}}$, and their dependence on $\eta \tan\theta_S$. From this figure we can see that $R_{\gamma\gamma}$ and $R_{b\bar{b}}$ follow a nearly linear correlation since now $\eta \tan\theta_S$ is very small, i.e. $|\eta \tan\theta_S| < 0.035$. One can also see that even with the requirement $|R| < 1\%$, $R_{b\bar{b}}$ and $R_{\gamma\gamma}$ may reach -10%. This is because the branching ratio of $h \to ss$ may still be moderate large under the constraint of current Higgs

data. Note that generally $|R_{\gamma\gamma}|$ is slightly larger than $|R_{b\bar{b}}|$, which can be understood by the positiveness of $\tan\theta_S$ in eq. (3.9).

4 Summary and conclusion

In this work, we intend to investigate the capability of the future Higgs factory such as TLEP in detecting the parameter space of the MDM, which extends the SM by one singlet scalar called dilaton. For this end, we calculate the Higgs-strahlung production process $e^+e^- \to Zh$ at the future Higgs factory by including radiative corrections in the model. We consider various theoretical and experimental constraints on the model, such as the vacuum stability, absence of Landau pole, the electro-weak precision data and the LHC search for Higgs boson, and perform fits to the Higgs data taken from ATLAS, CMS and CDF+D0. Then for the 1σ surviving samples, we investigate the MDM predictions on the inclusive production rate $\sigma(e^+e^- \to Zh)$ at the 240-GeV Higgs factory, and also the signal rates of $e^+e^- \to Zh$ with the Higgs boson decaying to $b\bar{b}$ and $\gamma\gamma$. We have following observations: (1) In the heavy dilaton scenario, the deviation of $\sigma(e^+e^- \to Zh)$ from its SM prediction can vary from -15% to 85%, which mainly arises from the modification of the tree-level hZZ coupling and also the radiative correction induced by possibly large Higgs self-couplings. (2) The processes $e^+e^- \to Zh$ at the Higgs factory and $pp \to hh$ at 14-TeV LHC are complementary in limiting the MDM parameter space. Requiring the deviation of $\sigma(e^+e^- \to Zh)$ from its SM prediction to be less than 1% and that of $\sigma(pp \to hh)$ to be less than 50%, $\tan\theta_S$ in the MDM will be limited to be $-0.1 < \tan\theta_S < 0.3$, the deviations of the signal rates are constrained to be $|R_{b\bar{b}}| < 2\%$ and $|R_{\gamma\gamma}| < 7\%$, and the Higgs self-coupling normalized to its SM prediction is upper bounded by about 4. (3) In the light dilaton scenario, the deviation of $\sigma(e^+e^- \to Zh)$ may reach -7%, and requiring its size to be less than 1% will result in $0 < \tan\theta_S < 0.1$, and $-10\% < R_{b\bar{b}}, R_{\gamma\gamma} < 1\%$.

References

[1] ATLAS collaboration, *Observation of a new particle in the search for the Standard Model Higgs boson with the ATLAS detector at the LHC*, *Phys. Lett.* **B 716** (2012) 1 [arXiv:1207.7214] [inSPIRE].

[2] CMS collaboration, *Observation of a new boson at a mass of* 125 *GeV with the CMS experiment at the LHC*, *Phys. Lett.* **B 716** (2012) 30 [arXiv:1207.7235] [inSPIRE].

[3] ATLAS collaboration, *Study of the spin of the new boson with up to* 25 fb^{-1} *of ATLAS data*, ATLAS-CONF-2013-040, CERN, Geneva Switzerland (2013).

[4] ATLAS collaboration, *Evidence for the spin-*0 *nature of the Higgs boson using ATLAS data*, *Phys. Lett.* **B 726** (2013) 120 [arXiv:1307.1432] [inSPIRE].

[5] CMS collaboration, *Study of the mass and spin-parity of the Higgs boson candidate via its decays to Z boson pairs*, *Phys. Rev. Lett.* **110** (2013) 081803 [arXiv:1212.6639] [inSPIRE].

[6] M. Carena, S. Gori, N.R. Shah and C.E.M. Wagner, *A* 125 *GeV SM-like Higgs in the MSSM and the* $\gamma\gamma$ *rate*, *JHEP* **03** (2012) 014 [arXiv:1112.3336] [inSPIRE].

[7] S. Heinemeyer, O. Stal and G. Weiglein, *Interpreting the LHC Higgs search results in the MSSM*, *Phys. Lett.* **B 710** (2012) 201 [arXiv:1112.3026] [inSPIRE].

[8] J. Cao, Z. Heng, D. Li and J.M. Yang, *Current experimental constraints on the lightest Higgs boson mass in the constrained MSSM*, *Phys. Lett.* **B 710** (2012) 665 [arXiv:1112.4391] [inSPIRE].

[9] N.D. Christensen, T. Han and S. Su, *MSSM Higgs bosons at the LHC*, *Phys. Rev.* **D 85** (2012) 115018 [arXiv:1203.3207] [inSPIRE].

[10] K. Hagiwara, J.S. Lee and J. Nakamura, *Properties of* 125 *GeV Higgs boson in non-decoupling MSSM scenarios*, *JHEP* **10** (2012) 002 [arXiv:1207.0802] [inSPIRE].

[11] P. Bechtle et al., *MSSM interpretations of the LHC discovery: light or heavy Higgs?*, *Eur. Phys. J.* **C 73** (2013) 2354 [arXiv:1211.1955] [inSPIRE].

[12] U. Ellwanger, *A Higgs boson near* 125 *GeV with enhanced di-photon signal in the NMSSM*, *JHEP* **03** (2012) 044 [arXiv:1112.3548] [inSPIRE].

[13] J.-J. Cao, Z.-X. Heng, J.M. Yang, Y.-M. Zhang and J.-Y. Zhu, *A SM-like Higgs near* 125 *GeV in low energy SUSY: a comparative study for MSSM and NMSSM*, *JHEP* **03** (2012) 086 [arXiv:1202.5821] [inSPIRE].

[14] U. Ellwanger and C. Hugonie, *Higgs bosons near* 125 *GeV in the NMSSM with constraints at the GUT scale*, *Adv. High Energy Phys.* **2012** (2012) 625389 [arXiv:1203.5048] [inSPIRE].

[15] J. Cao, Z. Heng, J.M. Yang and J. Zhu, *Status of low energy SUSY models confronted with the LHC* 125 *GeV Higgs data*, *JHEP* **10** (2012) 079 [arXiv:1207.3698] [inSPIRE].

[16] J.F. Gunion, Y. Jiang and S. Kraml, *The constrained NMSSM and Higgs near* 125 *GeV*, *Phys. Lett.* **B 710** (2012) 454 [arXiv:1201.0982] [inSPIRE].

[17] E. Hardy, J. March-Russell and J. Unwin, *Precision unification in* λSUSY *with a* 125 *GeV Higgs*, *JHEP* **10** (2012) 072 [arXiv:1207.1435] [inSPIRE].

[18] S.F. King, M. Mühlleitner and R. Nevzorov, *NMSSM Higgs benchmarks near* 125 *GeV*, *Nucl. Phys.* **B 860** (2012) 207 [arXiv:1201.2671] [inSPIRE].

[19] S.F. King, M. Mühlleitner, R. Nevzorov and K. Walz, *Natural NMSSM Higgs bosons*, *Nucl. Phys.* **B 870** (2013) 323 [arXiv:1211.5074] [inSPIRE].

[20] K. Agashe, Y. Cui and R. Franceschini, *Natural islands for a 125 GeV Higgs in the scale-invariant NMSSM*, *JHEP* **02** (2013) 031 [arXiv:1209.2115] [INSPIRE].

[21] BAYESFITS GROUP collaboration, K. Kowalska et al., *Constrained next-to-minimal supersymmetric Standard Model with a 126 GeV Higgs boson: a global analysis*, *Phys. Rev.* **D 87** (2013) 115010 [arXiv:1211.1693] [INSPIRE].

[22] T. Gherghetta, B. von Harling, A.D. Medina and M.A. Schmidt, *The scale-invariant NMSSM and the 126 GeV Higgs boson*, *JHEP* **02** (2013) 032 [arXiv:1212.5243] [INSPIRE].

[23] N.D. Christensen, T. Han, Z. Liu and S. Su, *Low-mass Higgs bosons in the NMSSM and their LHC implications*, *JHEP* **08** (2013) 019 [arXiv:1303.2113] [INSPIRE].

[24] M. Badziak, M. Olechowski and S. Pokorski, *New regions in the NMSSM with a 125 GeV Higgs*, *JHEP* **06** (2013) 043 [arXiv:1304.5437] [INSPIRE].

[25] S. Moretti, S. Munir and P. Poulose, *125 GeV Higgs boson signal within the complex NMSSM*, *Phys. Rev.* **D 89** (2014) 015022 [arXiv:1305.0166] [INSPIRE].

[26] S. Munir, L. Roszkowski and S. Trojanowski, *Simultaneous enhancement in $\gamma\gamma, b\bar{b}$ and $\tau^+\tau^-$ rates in the NMSSM with nearly degenerate scalar and pseudoscalar Higgs bosons*, *Phys. Rev.* **D 88** (2013) 055017 [arXiv:1305.0591] [INSPIRE].

[27] S. Munir, *Novel Higgs-to-125 GeV Higgs boson decays in the complex NMSSM*, *Phys. Rev.* **D 89** (2014) 095013 [arXiv:1310.8129] [INSPIRE].

[28] B. Bellazzini, C. Csáki, J. Hubisz, J. Serra and J. Terning, *A Higgslike dilaton*, *Eur. Phys. J.* **C 73** (2013) 2333 [arXiv:1209.3299] [INSPIRE].

[29] Z. Chacko, R. Franceschini and R.K. Mishra, *Resonance at 125 GeV: Higgs or dilaton/radion?*, *JHEP* **04** (2013) 015 [arXiv:1209.3259] [INSPIRE].

[30] D. Elander and M. Piai, *The decay constant of the holographic techni-dilaton and the 125 GeV boson*, *Nucl. Phys.* **B 867** (2013) 779 [arXiv:1208.0546] [INSPIRE].

[31] S. Matsuzaki and K. Yamawaki, *Is 125 GeV techni-dilaton found at LHC?*, *Phys. Lett.* **B 719** (2013) 378 [arXiv:1207.5911] [INSPIRE].

[32] S. Matsuzaki and K. Yamawaki, *Holographic techni-dilaton at 125 GeV*, *Phys. Rev.* **D 86** (2012) 115004 [arXiv:1209.2017] [INSPIRE].

[33] S. Matsuzaki and K. Yamawaki, *Discovering 125 GeV techni-dilaton at LHC*, *Phys. Rev.* **D 86** (2012) 035025 [arXiv:1206.6703] [INSPIRE].

[34] S. Matsuzaki and K. Yamawaki, *Techni-dilaton at 125 GeV*, *Phys. Rev.* **D 85** (2012) 095020 [arXiv:1201.4722] [INSPIRE].

[35] D.-W. Jung and P. Ko, *Higgs-dilaton(radion) system confronting the LHC Higgs data*, *Phys. Lett.* **B 732** (2014) 364 [arXiv:1401.5586] [INSPIRE].

[36] S. Dawson et al., *Working group report: Higgs boson*, arXiv:1310.8361 [INSPIRE].

[37] T. Han, Z. Liu and J. Sayre, *Potential precision on Higgs couplings and total width at the ILC*, *Phys. Rev.* **D 89** (2014) 113006 [arXiv:1311.7155] [INSPIRE].

[38] M.E. Peskin, *Estimation of LHC and ILC capabilities for precision Higgs boson coupling measurements*, arXiv:1312.4974 [INSPIRE].

[39] P. Bechtle, S. Heinemeyer, O. Stål, T. Stefaniak and G. Weiglein, *Probing the Standard Model with Higgs signal rates from the Tevatron, the LHC and a future ILC*, arXiv:1403.1582 [INSPIRE].

[40] M. Koratzinos et al., *TLEP: a high-performance circular e^+e^- collider to study the Higgs boson*, arXiv:1305.6498 [INSPIRE].

[41] TLEP DESIGN STUDY WORKING GROUP collaboration, M. Bicer et al., *First look at the physics case of TLEP*, *JHEP* **01** (2014) 164 [arXiv:1308.6176] [INSPIRE].

[42] T. Abe et al., *Minimal dilaton model*, *Phys. Rev.* **D 86** (2012) 115016 [arXiv:1209.4544] [INSPIRE].

[43] T. Abe et al., *Minimal dilaton model*, *Eur. Phys. J. Web Conf.* **49** (2013) 15018 [arXiv:1303.0935] [INSPIRE].

[44] J. Cao, Y. He, P. Wu, M. Zhang and J. Zhu, *Higgs phenomenology in the minimal dilaton model after run I of the LHC*, *JHEP* **01** (2014) 150 [arXiv:1311.6661] [INSPIRE].

[45] J. Baglio et al., *The measurement of the Higgs self-coupling at the LHC: theoretical status*, *JHEP* **04** (2013) 151 [arXiv:1212.5581] [INSPIRE].

[46] D.Y. Shao, C.S. Li, H.T. Li and J. Wang, *Threshold resummation effects in Higgs boson pair production at the LHC*, *JHEP* **07** (2013) 169 [arXiv:1301.1245] [INSPIRE].

[47] D. de Florian and J. Mazzitelli, *Two-loop virtual corrections to Higgs pair production*, *Phys. Lett.* **B 724** (2013) 306 [arXiv:1305.5206] [INSPIRE].

[48] D. de Florian and J. Mazzitelli, *Higgs boson pair production at next-to-next-to-leading order in QCD*, *Phys. Rev. Lett.* **111** (2013) 201801 [arXiv:1309.6594] [INSPIRE].

[49] L. Liu-Sheng et al., *NNLO QCD corrections to Higgs pair production via vector boson fusion at hadron colliders*, *Phys. Rev.* **D 89** (2014) 073001 [arXiv:1401.7754] [INSPIRE].

[50] J. Cao, Z. Heng, L. Shang, P. Wan and J.M. Yang, *Pair production of a 125 GeV Higgs boson in MSSM and NMSSM at the LHC*, *JHEP* **04** (2013) 134 [arXiv:1301.6437] [INSPIRE].

[51] Z. Heng, L. Shang and P. Wan, *Pair production of a 125 GeV Higgs boson in MSSM and NMSSM at the ILC*, *JHEP* **10** (2013) 047 [arXiv:1306.0279] [INSPIRE].

[52] D.T. Nhung, M. Mühlleitner, J. Streicher and K. Walz, *Higher order corrections to the trilinear Higgs self-couplings in the real NMSSM*, *JHEP* **11** (2013) 181 [arXiv:1306.3926] [INSPIRE].

[53] U. Ellwanger, *Higgs pair production in the NMSSM at the LHC*, *JHEP* **08** (2013) 077 [arXiv:1306.5541] [INSPIRE].

[54] C. Han, X. Ji, L. Wu, P. Wu and J.M. Yang, *Higgs pair production with SUSY QCD correction: revisited under current experimental constraints*, *JHEP* **04** (2014) 003 [arXiv:1307.3790] [INSPIRE].

[55] J. Liu, X.-P. Wang and S.-H. Zhu, *Discovering extra Higgs boson via pair production of the SM-like Higgs bosons*, arXiv:1310.3634 [INSPIRE].

[56] N. Haba, K. Kaneta, Y. Mimura and E. Tsedenbaljir, *Higgs pair production at the LHC and ILC from general potential*, *Phys. Rev.* **D 89** (2014) 015018 [arXiv:1311.0067] [INSPIRE].

[57] Q. Li, Q.-S. Yan and X. Zhao, *Higgs pair production: improved description by matrix element matching*, *Phys. Rev.* **D 89** (2014) 033015 [arXiv:1312.3830] [INSPIRE].

[58] Z. Heng, L. Shang, Y. Zhang and J. Zhu, *Pair production of 125 GeV Higgs boson in the SM extension with color-octet scalars at the LHC*, *JHEP* **02** (2014) 083 [arXiv:1312.4260] [INSPIRE].

[59] L. Wei-Hua et al., *Next-to-next-to-leading order QCD corrections to light Higgs pair production via vector boson fusion in type-II two-Higgs-doublet model*, arXiv:1403.2782 [INSPIRE].

[60] F. Goertz, A. Papaefstathiou, L.L. Yang and J. Zurita, *Higgs boson self-coupling measurements using ratios of cross sections*, *JHEP* **06** (2013) 016 [arXiv:1301.3492] [INSPIRE].

[61] R.S. Gupta, H. Rzehak and J.D. Wells, *How well do we need to measure the Higgs boson mass and self-coupling?*, *Phys. Rev.* **D 88** (2013) 055024 [arXiv:1305.6397] [INSPIRE].

[62] A.J. Barr, M.J. Dolan, C. Englert and M. Spannowsky, *Di-Higgs final states augMT2ed — selecting hh events at the high luminosity LHC*, *Phys. Lett.* **B 728** (2014) 308 [arXiv:1309.6318] [INSPIRE].

[63] V. Barger, L.L. Everett, C.B. Jackson and G. Shaughnessy, *Higgs-pair production and measurement of the triscalar coupling at LHC(8, 14)*, *Phys. Lett.* **B 728** (2014) 433 [arXiv:1311.2931] [INSPIRE].

[64] D.E. Ferreira de Lima, A. Papaefstathiou and M. Spannowsky, *Standard Model Higgs boson pair production in the $(b\bar{b})(b\bar{b})$ final state*, *JHEP* **08** (2014) 030 [arXiv:1404.7139] [INSPIRE].

[65] M. McCullough, *An indirect model-dependent probe of the Higgs self-coupling*, arXiv:1312.3322 [INSPIRE].

[66] S.L. Hu, N. Liu, J. Ren and L. Wu, *Probing Higgs couplings to diphoton and Z-photon from Higgs+photon production at a Higgs factory*, arXiv:1402.3050 [INSPIRE].

[67] ATLAS collaboration, *Search for pair production of heavy top-like quarks decaying to a high-p_T W boson and a b quark in the lepton plus jets final state in pp collisions at $\sqrt{s} = 8\, TeV$ with the ATLAS detector*, ATLAS-CONF-2013-060, CERN, Geneva Switzerland (2013).

[68] ATLAS collaboration, *Search for pair production of new heavy quarks that decay to a Z boson and a third generation quark in pp collisions at $\sqrt{s} = 8\, TeV$ with the ATLAS detector*, ATLAS-CONF-2013-056, CERN, Geneva Switzerland (2013).

[69] CMS collaboration, *Inclusive search for a vector-like T quark with charge $\frac{2}{3}$ in pp collisions at $\sqrt{s} = 8\, TeV$*, *Phys. Lett.* **B 729** (2014) 149 [arXiv:1311.7667] [INSPIRE].

[70] X.-F. Han, L. Wang, J.M. Yang and J. Zhu, *Little Higgs theory confronted with the LHC Higgs data*, *Phys. Rev.* **D 87** (2013) 055004 [arXiv:1301.0090] [INSPIRE].

[71] L. Wang, J.M. Yang and J. Zhu, *Dark matter in the little Higgs model under current experimental constraints from the LHC, Planck and Xenon data*, *Phys. Rev.* **D 88** (2013) 075018 [arXiv:1307.7780] [INSPIRE].

[72] J. Cao, F. Ding, C. Han, J.M. Yang and J. Zhu, *A light Higgs scalar in the NMSSM confronted with the latest LHC Higgs data*, *JHEP* **11** (2013) 018 [arXiv:1309.4939] [INSPIRE].

[73] A. Denner, J. Kublbeck, R. Mertig and M. Böhm, *Electroweak radiative corrections to $e^+e^- \to HZ$*, *Z. Phys.* **C 56** (1992) 261 [INSPIRE].

[74] N. Liu, J. Ren, L. Wu, P. Wu and J.M. Yang, *Full one-loop electroweak corrections to $e^+e^- \to ZH\gamma$ at a Higgs factory*, *JHEP* **04** (2014) 189 [arXiv:1311.6971] [INSPIRE].

[75] C. Englert and M. McCullough, *Modified Higgs sectors and NLO associated production*, *JHEP* **07** (2013) 168 [arXiv:1303.1526] [INSPIRE].

[76] PARTICLE DATA GROUP collaboration, J. Beringer et al., *Review of particle physics (RPP)*, *Phys. Rev.* **D 86** (2012) 010001 [INSPIRE].